

# Comparative Analysis of Argonaute-Dependent Small RNA Pathways in *Drosophila*

Rui Zhou,<sup>1,5</sup> Ikuko Hotta,<sup>2,3,5</sup> Ahmet M. Denli,<sup>2</sup> Pengyu Hong,<sup>4</sup> Norbert Perrimon,<sup>1,\*</sup> and Gregory J. Hannon<sup>2,\*</sup>

<sup>1</sup>Department of Genetics, Harvard Medical School, Howard Hughes Medical Institute, Boston, MA 02115, USA

<sup>2</sup>Watson School of Biological Sciences, Howard Hughes Medical Institute, Cold Spring Harbor Laboratory, Cold Spring Harbor, NY 11724, USA

<sup>3</sup>Graduate Program in Molecular and Cellular Biology, State University of New York at Stony Brook, Stony Brook, NY 11794, USA

<sup>4</sup>Department of Computer Science, Brandeis University, MS018, Waltham, MA 02454, USA

<sup>5</sup>These authors contributed equally to this work

\*Correspondence: [perrimon@receptor.med.harvard.edu](mailto:perrimon@receptor.med.harvard.edu) (N.P.), [hannon@cshl.edu](mailto:hannon@cshl.edu) (G.J.H.)

DOI 10.1016/j.molcel.2008.10.018

## SUMMARY

The specificity of RNAi pathways is determined by several classes of small RNAs, which include siRNAs, piRNAs, endo-siRNAs, and microRNAs (miRNAs). These small RNAs are invariably incorporated into large Argonaute (Ago)-containing effector complexes known as RNA-induced silencing complexes (RISCs), which they guide to silencing targets. Both genetic and biochemical strategies have yielded conserved molecular components of small RNA biogenesis and effector machineries. However, given the complexity of these pathways, there are likely to be additional components and regulators that remain to be uncovered. We have undertaken a comparative and comprehensive RNAi screen to identify genes that impact three major Ago-dependent small RNA pathways that operate in *Drosophila* S2 cells. We identify subsets of candidates that act positively or negatively in siRNA, endo-siRNA, and miRNA pathways. Our studies indicate that many components are shared among all three Argonaute-dependent silencing pathways, though each is also impacted by discrete sets of genes.

## INTRODUCTION

Despite similarities in their form and overall function, small RNAs that bind Argonaute (Ago) proteins in *Drosophila* arise from compartmentalized biogenesis pathways and join effector complexes with specialized properties (Zamore and Haley, 2005). *Drosophila* small interfering RNAs (siRNAs) are most often generated from exogenously introduced double-stranded RNAs (dsRNAs), though the replication products of RNA viruses can enter this pathway (Wang et al., 2006). Double-stranded RNA can also be produced from the *Drosophila* genome itself, either from loci encoding extensively structured RNAs or by hybridization of convergently transcribed mRNAs (Czech et al., 2008; Ghildiyal et al., 2008; Kawamura et al., 2008; Okamura et al., 2008). These bind Ago2 to form a complex that can efficiently cleave complemen-

tary targets. miRNAs are generated via a two-step processing pathway from endogenously transcribed primary miRNAs (pri-miRNAs). miRNAs guide Ago1 via a 5' "seed" sequence to mRNA targets, which are primarily repressed at the translational level (Bartel, 2004).

A great deal of progress has been made in deciphering small RNA-based regulatory networks; however, it is clear that many additional components are pending identification and functional characterization. Genome-scale screens for components of siRNA or miRNA pathways have been carried out, with some overlap between components identified (Dorner et al., 2006; Eulalio et al., 2007; Kim et al., 2005; Parry et al., 2007; Saleh et al., 2006; Ulvila et al., 2006). However, none of these screens have addressed endo-siRNA pathways, nor have they attempted comparative studies in the same experimental model. Here, we report comparative and comprehensive RNAi screens that identify components of the Argonaute-dependent small RNA pathways (siRNA, miRNA, and endo-siRNA) in cultured *Drosophila* cells.

## RESULTS

### Assay Systems to Monitor the siRNA/miRNA Pathways

We constructed robust assay systems that allowed us to interrogate the miRNA and siRNA pathways individually. For probing the siRNA pathway, we created an S2 cell line (RZ-14) stably expressing both the *Renilla* luciferase and a 688 bp perfect inverted repeat that directs *Renilla* silencing (Figure S1A available online). To identify components of the miRNA pathway, we embedded an artificial miRNA sequence (CXCR4) into the Bantam pri-miRNA (Figure S1B). This construct was transiently introduced into S2 cells together with an expression construct for a *Renilla* luciferase gene with multiple imperfect CXCR4 complementary sites in its 3' UTR (Doench et al., 2003). In both assays, an expression construct for the firefly luciferase gene served as a normalization control. To prevent the half-life of reporter proteins from confounding our analysis, all transgenes were expressed from the inducible *metallothionein* promoter.

Both assays systems performed as expected upon knockdown of known components of either pathway. Silencing of *Dcr-2* or *Ago2* caused significant derepression of siRNA reporters, whereas dsRNAs against *Droscha*, *Dcr-1*, or *Ago1* had no effect (Figure S1C). Conversely, depletion of *Droscha* or *Ago1* led to

a marked decrease in miRNA-mediated gene silencing, while treatment with dsRNAs against *LacZ*, *Dcr-2*, or *Ago2* had no effect (Figure S1D).

### Comprehensive Identification of siRNA/miRNA Pathway Components

We screened a collection of ~21,000 dsRNAs for those that impacted the siRNA and miRNA pathways. To assess reproducibility, dsRNAs targeting each positive emerging from the two primary screens were resynthesized and tested multiple times using both assay systems. To minimize potential off-target effects, we also generated additional independent dsRNAs targeting each gene and assessed their impacts on the siRNA and miRNA pathways. Only genes represented by two or more independent consistently scoring dsRNAs were selected as final candidates. We found that *Dcr-2* and *Ago2* were among the siRNA pathway genes, whereas *Drosha* and *Ago1* were among the miRNA pathway candidates (Figure 1C and Table S1), providing an internal validation of each screen.

Recently, an extensive collection of endogenous siRNAs has been characterized in *Drosophila* (Czech et al., 2008; Ghildiyal et al., 2008; Kawamura et al., 2008; Okamura et al., 2008). The biogenesis and function of these endo-siRNAs depend upon canonical RNAi pathway components, including *Dcr-2* and *Ago2*. In some cases, endo-siRNA production depends much more heavily on Loquacious rather than on the canonical *Dcr-2* partner, *R2D2* (Czech et al., 2008; Okamura et al., 2008). We tested all candidates emerging from the miRNA and siRNA pathway screens for their impacts on a sensor for an abundant endo-siRNA, esi-2.1 (Figure S1E). In summary, 177 candidates were identified that affected at least one of the three pathways when knocked down (Figure 1A). Among the 116 candidates for the siRNA pathway, 84 also altered the endo-siRNA pathway, and 70 altered the miRNA pathway. Significant overlap (69) was also observed between the endo-siRNA (132) and miRNA pathway (98) candidates. Notably, 54 candidates affected all three pathways.

### Candidate Genes Identified from the Screens

Based on their annotations, candidates that affect small RNA pathways could be assigned to several functional categories. Notably, genes encoding RNA-binding/processing factors and translation factors were enriched by ~10-fold (Figure 1B), since only ~2% of all *Drosophila* genes belong to this class (Lasko, 2000). These included splicing factors, RNA helicases, and proteins involved in polyadenylation. Splicing factors could have scored in the siRNA pathway screen because the artificial hairpin transcript, which triggers silencing, carries an intron. However, neither the miRNA expression construct nor the endo-siRNA triggers contain intronic sequences, yet most splicing factors still impacted their function. Moreover, in a screen for RNAi pathway components in *C. elegans*, a number of splicing factors, as well as the ortholog of the U1-associated factor, PSI, were identified (Kim et al., 2005).

Many candidates emerging from the screens showed direct protein-protein interactions, fit into functional modules, or joined known multiprotein complexes (Tables S1 and S2). For example, six U2 snRNP proteins displayed a similar scoring pattern in the screen. We also observed common behavior for two U1 snRNP

proteins, snRNP70K and CG5454, and for PSI, which physically and functionally interacts with snRNP70K (Labourier et al., 2001; Salz et al., 2004).

Knockdown of several ribosomal proteins impacted small RNA pathways. While this effect could be indirect, some ribosomal proteins have been implicated in the siRNA pathway. For example, RpL11 and RpL5 have been shown to reside in a protein complex containing FMR, Dmp68, and Ago2 in S2 cells (Ishizuka et al., 2002).

Silencing a number of proteasomal components consistently impacted all three small RNA pathways. Indeed, a regulatory subunit, Pros45, has previously been implicated in RNAi (Ulvila et al., 2006). We find that knockdown of Tbp-1, CG12000, or l(2)05070 led to a decrease in miRNA-mediated silencing and a concomitant reduction in miRNA levels (Figure 2A). It is not yet clear whether these effects are direct or indirect.

### Placing Candidates within the siRNA/miRNA Pathway

Candidates affecting the miRNA pathway could impact miRNA biogenesis/stability or miRNA effector functions. To map candidates along the pathway, we examined the effects of their knockdown on steady-state levels of the CXCR4 miRNA mimetic, on endogenous miR-2b, and on those of pri-CXCR4. Knockdown of several candidates led to consistent alterations in mature miRNA levels that paralleled effects on miRNA-mediated silencing (Figure 2A and Table S3). For example, *Drosha* and *Ago1* silencing reduced both miRNA levels and miRNA function, and *Drosha* silencing also led to a coincidental accumulation of pri-CXCR4. This class of positives likely affects miRNA processing and/or stability. Unexpectedly, silencing of *Ago1* also had an impact on pri-miRNA levels. While this could represent a feedback mechanism, it is also possible that a miRNA indirectly regulates the *metallothionein* promoter used to express the pri-CXCR4 in this study. Another set of candidates (such as CG5514, CG3814, and CG2807) impacted miRNA-mediated repression without corresponding effects on mature miRNA levels. These positives most likely impact directly or indirectly effector steps within the pathway.

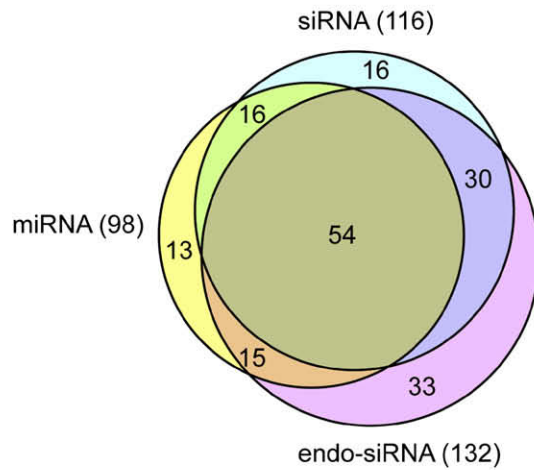
We also examined steady levels of esi-2.1 upon knockdown of candidates. As shown in Figure 2B, knockdown of a group of candidates (e.g., CG7185 and snRNP70K) caused a decrease in esi-2.1-mediated gene silencing, which correlates with a reduction in esi-2.1 levels. This suggests involvement in siRNA production and/or stability. In contrast, knockdown of *ubi-p63E*, CG11700, or CG12000 caused a change in esi-2.1 activity that did not correlate with alterations in esi-2.1 RNA levels. Considered together, our analyses of the steady-state levels of small RNAs and their precursors following candidate knockdown provide clues on the placement of candidates within small RNA pathways.

### Validation of Belle as a Bona Fide RNAi Pathway Component

*belle* (*bel*) emerged from our screen and from other studies as an RNAi pathway candidate (Kim et al., 2005; Ulvila et al., 2006). It encodes a DEAD-box RNA helicase, which is required for viability and in the germ line (Johnstone et al., 2005). We chose to validate *bel* both in animals and through biochemical approaches.

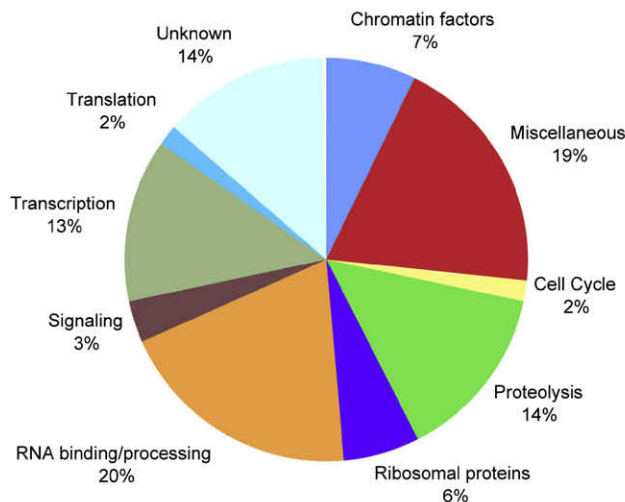
A

Total number of candidate genes: 177

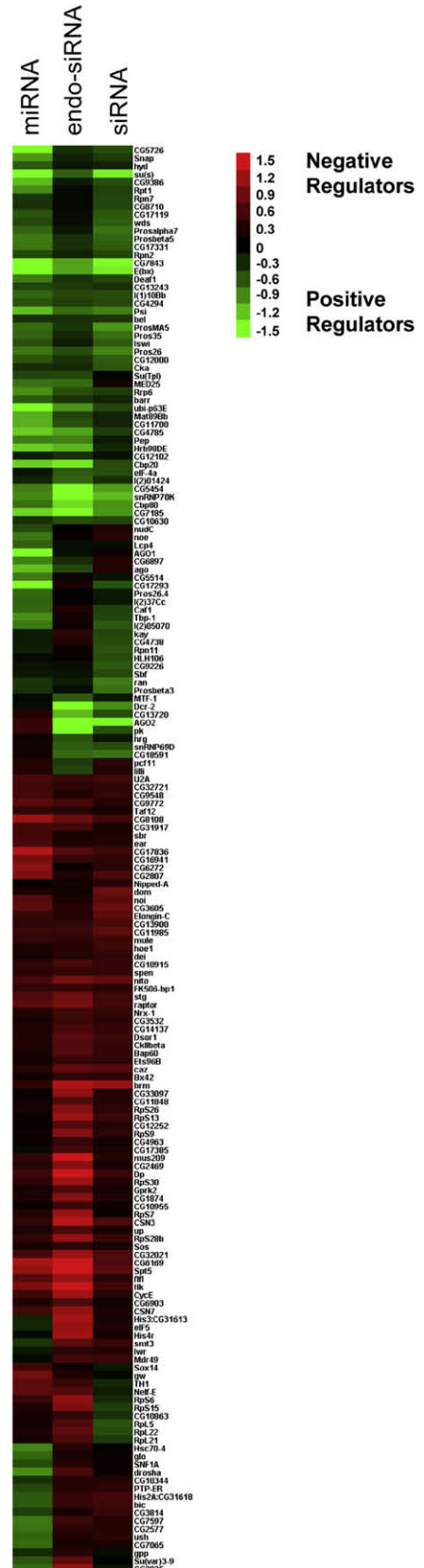


- siRNA only (16)
- endo-siRNA only (33)
- miRNA only (13)
- siRNA & endo-siRNA, but not miRNA (30)
- siRNA & miRNA, but not endo-siRNA (16)
- miRNA & endo-siRNA, but not siRNA (15)
- siRNA, miRNA & endo-siRNA (54)

B



C



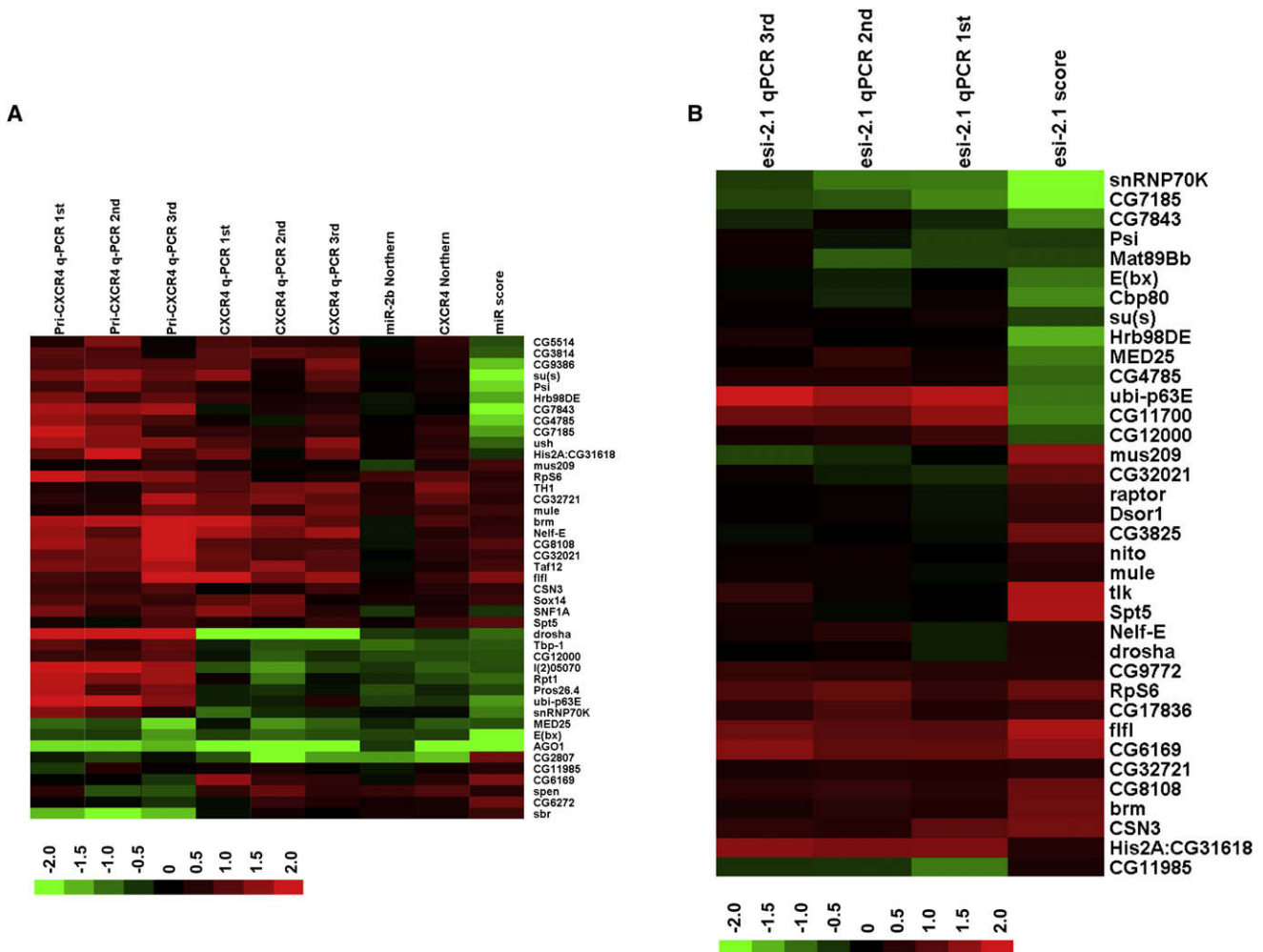


**Figure 2. Mapping Candidates along the Small RNA Pathway**

(A) A heat map of steady-state pri-miRNA and miRNA levels upon knockdown of candidates. Steady-state levels of CXCR4 and those of endogenous miR-2b upon knockdown of 43 selected candidates were examined by northern blotting and semiquantitative RT-PCR (q-PCR). miRNA levels were quantified and normalized first against U6 RNA levels and then against the average of multiple controls (cells treated with dsRNA against LacZ). Also shown are steady-state levels of pri-CXCR4 measured by q-PCR and the relative miRNA pathway activities associated with the representative dsRNA. Red indicates an increase in RNA levels or an increase in the activity of the miRNA pathway, and green indicates a decrease. Presented are the average from two to four independent northern blotting experiments and results from individual independent q-PCR assays. The scores associated with each candidate were from experiments involving one representative dsRNA targeting that gene (Table S3).

(B) A heat map of endo-siRNA levels upon knockdown of candidates. Steady-state levels of esi-2.1 upon knockdown of 36 selected candidates were examined by q-PCR using multiple independent RNA samples. Quantification was performed as described in (A). Also shown are the relative esi-2.1-mediated gene silencing activities. The scores associated with each candidate were from experiments involving one representative dsRNA (Table S4).

In order to assess RNAi efficiency in flies, we used transgenics carrying an inverted repeat of the *white* (*w*) gene under the control of the eye-specific *GMR* promoter (*GMR-wIR*; Figure 3). These flies display a pale eye color due to strong suppression of *white*.

Because *bel* is essential, we used an eye-specific mitotic recombination system to generate mosaics in which we could assay the impact of a *bel* allele (*bel<sup>6</sup>*) on *w* silencing in clones (Stowers and Schwarz, 1999). As previously described, eye cells homozygous

**Figure 1. Candidates Identified from the Screens**

(A) A Venn diagram showing the impact of the candidates on the siRNA, endo-siRNA, and miRNA assays.

(B) Candidates were sorted into various categories based on their annotated/verified function.

(C) A heat map of the candidates and their scoring patterns in multiple assays. The scores assigned to individual genes in a given assay reflect the relative activity of the pathway upon knockdown of candidate gene expression. Red indicates an increase in silencing, and green indicates a decrease. As each candidate is represented by multiple independent dsRNAs, presented are the average scores from all independent dsRNAs targeting a given gene. Scores for individual dsRNAs are shown in Table S1.

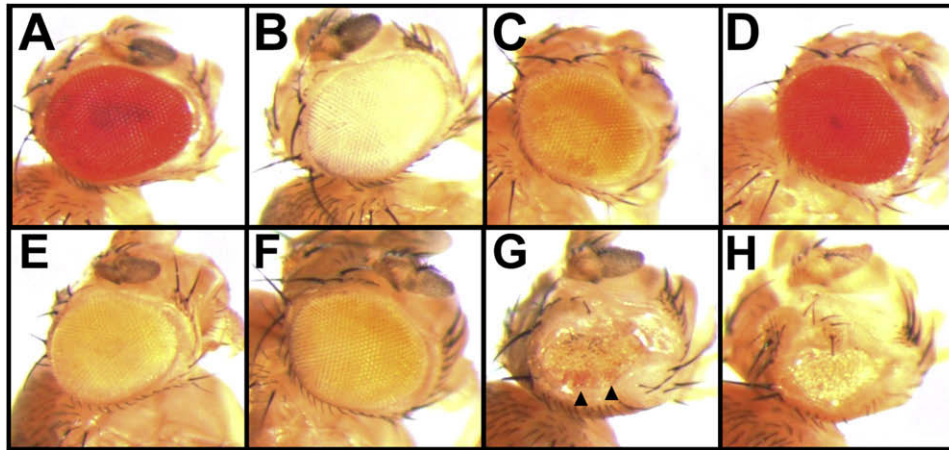


**Figure 3. *bel*<sup>6</sup> Flies Are Defective in RNAi**

Eye phenotypes of the corresponding genotypes are shown.

(A) *Ore<sup>R</sup>*

(B) *w<sup>1118</sup>*

(C) *w<sup>+</sup>, GMR-wIR/yw; dcr-2<sup>L811fsX</sup>, FRT42D/CyO; EGFU/+*

(D) *w<sup>+</sup>, GMR-wIR/yw; dcr-2<sup>L811fsX</sup>, FRT42D/FRT42D, GMR-hid, Ci; EGFU/+*

(E) *w<sup>+</sup>, GMR-wIR/yw; EGFU/+; FRT82B/FRT82B, Ci, GMR-hid*

(F) *w<sup>+</sup>, GMR-wIR/yw; EGFU/+; bel<sup>6</sup>, FRT82B/TM2*

(G) *w<sup>+</sup>, GMR-wIR/yw; EGFU/+; bel<sup>6</sup>, FRT82B/FRT82B, Ci, GMR-hid*

(H) *w<sup>+</sup>, GMR-wIR/yw; EGFU/+; hsc70-4<sup>54.1</sup>, FRT82B/FRT82B, Ci, GMR-hid*

for a *Dcr-2* mutation, *Dcr-2<sup>fsL811X</sup>*, display a dark red color, indicating loss of silencing (Figure 3D; Lee et al., 2004). Eyes predominantly homozygous for *bel*<sup>6</sup> are rough and small, suggesting that *bel* is required for cell viability. Importantly, patches of cells with increased pigmentation are observed in homozygous *bel*<sup>6</sup> clones (Figure 3G, arrowheads). We examined *hsc70-4* mutant eyes, which are also small and rough, and found pigmentation to be unaffected, suggesting that the *bel*<sup>6</sup> phenotype is specific (Figure 3H). These observations suggest that *bel*<sup>6</sup> mutant clones are defective in RNAi.

Next, we tested whether Bel associates with RNAi components. Cytoplasmic extract was prepared from S2 cells and fractionated by gel filtration. Individual fractions were immunoblotted using antibodies against Bel and components of RISC, including VIG, FMR, Ago2, or Ago1. The majority of Bel cofractionates with Ago1, whereas a smaller fraction coelutes with Ago2, FMR, and VIG, components of the siRISC (Figure 4A). We also immunoprecipitated FLAG-tagged Bel from S2 cells and found robust coprecipitation of Ago2, FMR, or VIG (Figure 4B). RNase treatment reduced interaction with Ago2 and VIG, but not as substantially with FMR (Figure 4B).

To test interactions of Bel with small RNAs, we expressed FLAG-tagged Bel or known components of the RISC together with an artificial siRNA (CXCR4) generated from a perfectly complementary hairpin expression construct. As expected, robust CXCR4 signals could be detected in the Ago2 or VIG complexes (Figure 4C). Importantly, CXCR4 was also present in the Bel immunoprecipitate, as was esi-2.1, though they are probably bound directly to another protein in the complex. We conclude that Bel likely acts directly as part of the RNAi machinery, as it resides in a complex that also contains both protein and RNA

components of RISC. Interestingly, more CXCR4 siRNA was present in the Ago1 immunoprecipitate than was detected in the Ago2 sample (Figure 4C). While this could be attributed to some intrinsic characteristics of the CXCR4 siRNA mimetic, it is also possible that the coupling between miRNA processing and loading steps accounts for this observation.

#### Ribosomal Proteins Associate with the RNAi Machinery

We found that Rpl22, a candidate from the screen, could coimmunoprecipitate components of the siRISC, including VIG, FMR, and Ago2, suggesting either a direct or indirect interaction. Similar behavior was observed for several other ribosomal proteins (Figure 4B). These interactions seemed to display different degrees of dependence on RNA. For example, RNase treatment caused a moderate decrease in the levels of Ago2 in the Rpl22 immunoprecipitate, whereas the levels of FMR and VIG remained unaffected (Figure 4B). Similar observations were also made for the Rps7 and Rpl21 samples. Moreover, both CXCR4 and esi-2.1 are present in the immunoprecipitates of a number of ribosomal proteins, including Rpl22, Rps7, Rpl21, and Rpl49 (Figure 4C). These observations indicate that these ribosomal proteins reside in large RNA protein complex(es) that also contain core components of the RNAi machinery.

#### DISCUSSION

In *Drosophila*, siRNA and miRNA pathways have been viewed as being biochemically compartmentalized. However, the boundary between these pathways has been blurred by recent observations that, depending on the configuration of their precursors, miRNAs (and possibly siRNAs) can be partitioned between

Ago1 and Ago2 (Forstemann et al., 2007; Tomari et al., 2007). Moreover, Loquacious plays roles both in miRNA biogenesis and in the production of some endo-siRNAs (Czech et al., 2008; Okamura et al., 2008). Intimate connections between siRNA and miRNA pathways are also suggested by the observation that knockdown of Ago2 leads to more pronounced silencing by miRNAs (Figure 1C), possibly by increasing the access of Ago1 to miRNAs or other limiting components that were previously bound by Ago2.

Analysis of miRNA and siRNA screens shows extensive overlap between genes that impact these pathways. Suppression of many candidates reduces the efficiency of the target small RNA pathways, indicating that those genes might be components of siRNA- or miRNA-mediated responses. Silencing of a roughly equal number of genes increases silencing, indicating that they encode negative regulators of small RNA pathways. These so-called “enhancer of RNAi” phenotypes might indicate attractive targets for genetic manipulation or small molecule inhibitors that could increase the activity of RNAi in either experimental or therapeutic settings. It is worth noting that our analysis of steady-state levels of small RNAs upon candidate knockdown revealed that, for some, enhanced silencing is correlated with increased levels of the small RNA silencing trigger, as is the case for the miRNA pathway candidates such as *CG32721*, *mule*, *TH1*, or *fff1* (Figure 2A). In contrast, while knocking down *CG2807* led to markedly enhanced silencing by the miRNA mimetic CXCR4, the steady-state levels of both CXCR4 and miR-2b significantly decreased. While these effects on the small RNA pathways could be indirect, these observations suggest that some of these negative regulators of RNAi are primarily involved in the biogenesis and/or stability of the small RNA silencing trigger, while others are implicated in the downstream effector steps.

Each pathway was uniquely or differentially affected by a number of genes (Figure 1C). For example, knockdown of one class of genes (*caf1*, *CG17293*, and genes encoding ribosomal proteins L5, L21, L22, and S15) led to decreased silencing by exogenous siRNAs but enhanced silencing by endo-siRNAs. Suppression of such a class of genes might enhance the production or loading of endo-siRNAs into RISC, thereby depleting the pool available for products of exogenously introduced dsRNAs, a model that has been previously proposed for some loci in *C. elegans* (Duchaine et al., 2006). Knockdown of another group of genes (*hsc70-4*, *CG3825*, and *CG2577*) decreased silencing by miRNAs but enhanced silencing by endo-siRNAs. A number of possibilities, including effects on small RNA sorting, might account for these observations.

We validated Bel as a bona fide component of the RNAi pathway. Bel most likely functions at step(s) downstream of siRNA processing and loading, as neither steady-state levels of esi-2.1 nor the levels of Ago2-bound esi-2.1 are affected by Bel knockdown (Figures S2 and S3). Interestingly, Ago1 and Bantam are also present in the Bel immunoprecipitate, consistent with the cofractionation of Bel with miRISC (Figures 4B and 4C). Thus, Bel may also participate in the miRNA pathway. While none of the *bel* dsRNAs met the scoring criteria in the miRNA assay, they did trend consistently (Table S1).

Ago1 and Bantam were present in a number of ribosomal protein immunoprecipitates, and the association between Ago1 and

these ribosomal proteins was abolished by RNase treatment (Figures 4B and 4C). These observations are consistent with the notion that miRISC associates with the translation machinery. Both protein and RNA components of the siRISC are also present in these immunoprecipitates, and that knockdown of a number of ribosomal proteins consistently leads to enhanced silencing by endo-siRNAs (Table S1). Thus, the integrity and function of the translational machinery as a whole may be impacting the small RNA pathways.

In summary, our comparative genome-wide screens (Table S5) generate a rich resource for further study of the three Argonaute-dependent small RNA regulatory pathways in *Drosophila*. These studies not only point to extensive overlap and interplay among small RNA directed silencing machineries in flies but also highlight specific players in each of the three pathways.

## EXPERIMENTAL PROCEDURES

### DNA Constructs and Cell Culture

Detailed description of DNA constructs can be found in the Supplemental Experimental Procedures. S2-NP cells were maintained in Schneider's medium (Invitrogen) supplemented with 10% FBS and 1% pen-strep (Invitrogen). To generate the RZ-14 stable cell line, S2-NP cells were transfected with pRmHa-3-Firefly-long, pRmHa-3-*Renilla*, and pRmHa-3-*Renilla*-hairpin together with pHS-neo, using Effectene (QIAGEN). Transfected cells were selected and maintained in growth medium supplemented with 400  $\mu$ g/ml G418.

### RNAi Screening

Detailed description of the RNAi screening and bioinformatic analysis can be found in the Supplemental Experimental Procedures.

### RNA Isolation, Northern Blotting, and q-PCR Assays

S2-NP cells were transiently transfected with DNA constructs for the miRNA assay (pMT-*Renilla*-CXCR4-6B, pMT-D05, and pRmHa-3-Firefly-long). Two days after transfection,  $\sim 3 \times 10^6$  cells were incubated in 1.5 ml serum-free Schneider's medium containing 10  $\mu$ g of candidate dsRNAs in 6-well plates, and 3 ml serum-containing medium was added 45 min later. After 3 days of dsRNA treatment, cells were induced with 200 mM CuSO<sub>4</sub> for 24 hr. A small aliquot of cells were subjected to luciferase assays to examine the effect of dsRNA treatment on reporter activity. Total RNAs were extracted from the rest of the samples using Trizol (Invitrogen). Northern blotting was performed as previously described (Czech et al., 2008). miRNA signals were normalized against that of the U6 RNA. A score was assigned to each sample based on the average results from two or four independent experiments. To quantify steady-state levels of pri- and mature miRNAs, semiquantitative RT-PCR (q-PCR) assays were performed (Applied Biosystems) using primers specific for pri-Bantam, CXCR4, and U6.

### Immunoprecipitation of Proteins and RNAs

Cells were transfected with expression constructs for epitope-tagged proteins, induced with 500  $\mu$ M CuSO<sub>4</sub> 2 days after transfection, and harvested another 24 hr later. Immunoprecipitation was performed as described (Czech et al., 2008). For RNase treatment, the immunoprecipitates were split into two sets, and one was incubated in lysis buffer with 100  $\mu$ g/ml RNase A at 4°C for 15 min prior to washing. For RNA immunoprecipitation, cells were transfected with protein expression constructs together with pMT-F12, an expression vector for CXCR4 derived from a perfectly base-paired precursor, and induced with 500  $\mu$ M CuSO<sub>4</sub> 2 days after transfection. Cells were harvested and cell lysates prepared 24 hr later. About 80% of the cell lysates were subject to immunoprecipitation using M2 agarose beads. After washing, 10% of the immunoprecipitates were analyzed by western blotting to verify the expression of the epitope-tagged proteins. Total RNAs were extracted from the remaining immunoprecipitates and cell lysates and analyzed by northern blotting.

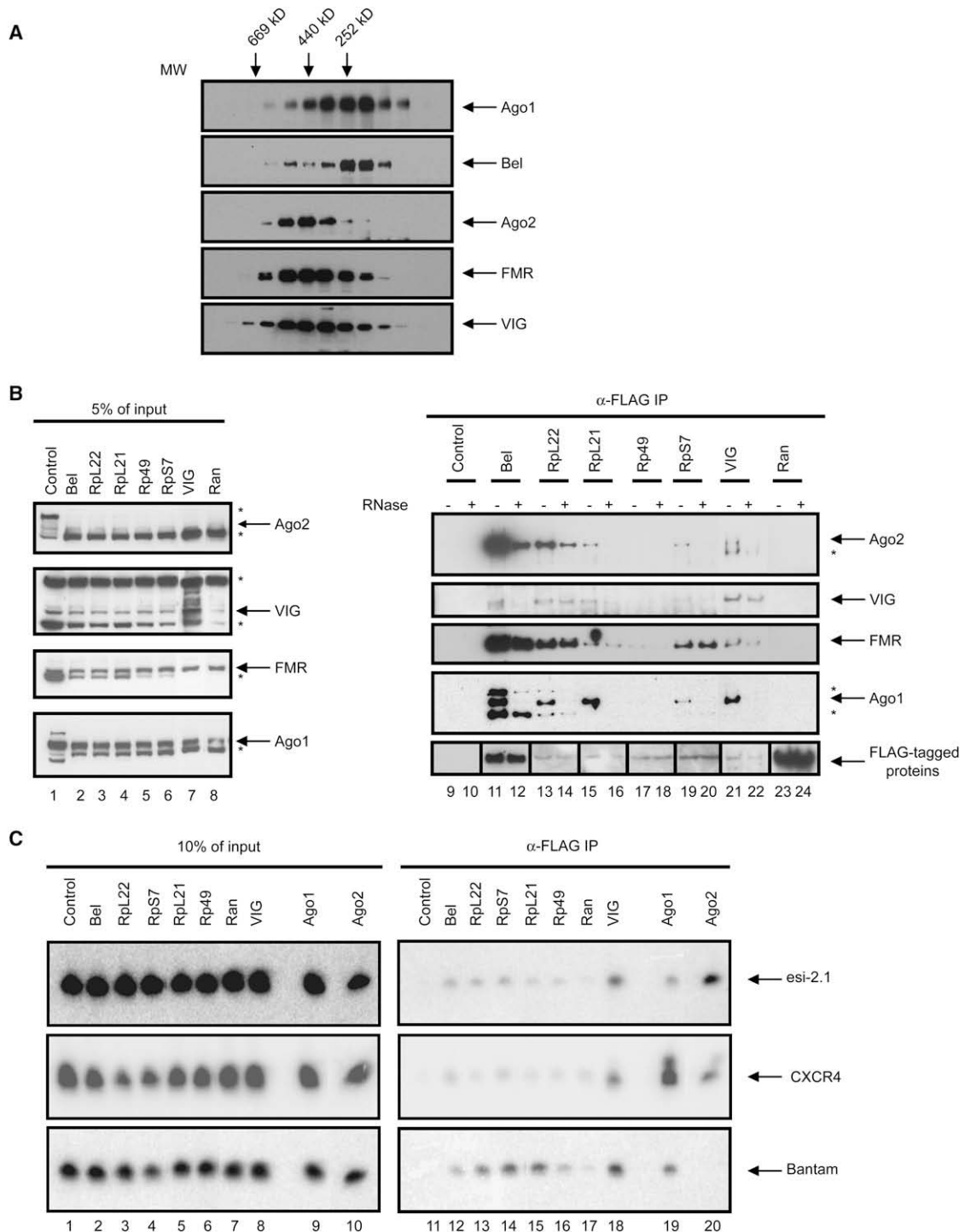


**Figure 4. Bel and RpL22 Interact with Components of the RISC**

(A) Cytoplasmic extract from S2-NP cells was fractionated by size exclusion chromatography, and the fractions were immunoblotted using antibodies against Bel and components of the RNAi pathway, as indicated. The elution profile of molecular markers is shown on top of the panel.

(B) FLAG-tagged proteins (as labeled above the panel) were expressed in S2-NP cells, and anti-FLAG immunoprecipitates were prepared. The samples were evenly split, and one set was treated with RNase, while the other served as control. The samples were immunoblotted sequentially using antibodies against VIG, Ago2, FMR, Ago1, and FLAG. A small amount of cell extract was processed in parallel as input control. Nonspecific bands are marked with an asterisk. Note that the images shown in lanes 9 through 12 and 23 through 24 of the anti-FLAG panel were from films that were subjected to different exposure times from the rest due to differences in expression levels.

**Size Exclusion Chromatography**

S2-NP cells were lysed in hypotonic buffer (20 mM HEPES [pH 7.0], 2 mM MgCl<sub>2</sub>, 0.2 mM CaCl<sub>2</sub>, 1 mM DTT) and spun at 30,000 × g for 20 min. The supernatant was spun at 200,000 × g for 2.5 hr, and the resulting pellet was subsequently resuspended in buffer A (20 mM HEPES [pH 7.0], 2 mM MgCl<sub>2</sub>, 0.2 mM CaCl<sub>2</sub>, 1 mM DTT, 0.5% octyl glucoside, 400 mM KCl) and spun at 200,000 × g for another 2.5 hr. The supernatant was fractionated on Superose-6 HR10/10 (Pharmacia).

**Fly Stocks**

*bel* mutant flies (*bel<sup>f</sup>*) were from the Bloomington stock center and from Dr. Paul Lasko; *EGUF* flies were from the Bloomington stock center and from Drs. Thomas Schwarz and Stephen Stowers; and the *GMR-wlR* and *dcr-2<sup>L811fsX</sup>* flies were from Drs. Richard Carthew and Sara Cherry.

**SUPPLEMENTAL DATA**

The Supplemental Data include Supplemental Experimental Procedures, three figures, and five tables and can be found with this article online at [http://www.molecule.org/supplemental/S1097-2765\(08\)00734-X](http://www.molecule.org/supplemental/S1097-2765(08)00734-X).

**ACKNOWLEDGMENTS**

We thank members of the Hannon and Perrimon labs, especially Sara Cherry for helpful discussion and Julius Brennecke, Ben Czech, and Colin Malone for sharing unpublished data and reagents. We also thank the DRSC staff for technical support, the Bloomington stock center, and Drs. Paul Lasko, Thomas Schwarz, Stephen Stowers, Richard Carthew, and Sara Cherry for fly stocks. We are grateful to Dr. Phillip Sharp for the CXCR4 constructs and to Dr. Paul Lasko for the *Bel* antibody. We are indebted to Drs. Bernard Mathey-Prevot and Richard Binari for critically reading the manuscript. R.Z. is supported by a Special Fellowship from the Leukemia and Lymphoma Society. This work was supported by grants from the NIH (P.H., N.P., and G.J.H.) and by a kind gift from K.W. Davis (G.J.H.). N.P. and G.J.H. are investigators of the Howard Hughes Medical Institute.

Received: June 15, 2008

Revised: September 16, 2008

Accepted: October 28, 2008

Published: November 20, 2008

**REFERENCES**

Bartel, D.P. (2004). MicroRNAs: genomics, biogenesis, mechanism, and function. *Cell* 116, 281–297.

Czech, B., Malone, C.D., Zhou, R., Stark, A., Schlingeheyde, C., Dus, M., Perrimon, N., Kellis, M., Wohlschlegel, J.A., Sachidanandam, R., et al. (2008). An endogenous small interfering RNA pathway in *Drosophila*. *Nature* 453, 798–802.

Doench, J.G., Petersen, C.P., and Sharp, P.A. (2003). siRNAs can function as miRNAs. *Genes Dev.* 17, 438–442.

Dorner, S., Lum, L., Kim, M., Paro, R., Beachy, P.A., and Green, R. (2006). A genome-wide screen for components of the RNAi pathway in *Drosophila* cultured cells. *Proc. Natl. Acad. Sci. USA* 103, 11880–11885.

Duchaine, T.F., Wohlschlegel, J.A., Kennedy, S., Bei, Y., Conte, D., Jr., Pang, K., Brownell, D.R., Harding, S., Mitani, S., Ruvkun, G., et al. (2006). Functional proteomics reveals the biochemical niche of *C. elegans* DCR-1 in multiple small-RNA-mediated pathways. *Cell* 124, 343–354.

Eulalio, A., Rehwinkel, J., Stricker, M., Huntzinger, E., Yang, S.F., Doerks, T., Dorner, S., Bork, P., Boutros, M., and Izaurralde, E. (2007). Target-specific requirements for enhancers of decapping in miRNA-mediated gene silencing. *Genes Dev.* 21, 2558–2570.

Forstemann, K., Horwich, M.D., Wee, L., Tomari, Y., and Zamore, P.D. (2007). *Drosophila* microRNAs are sorted into functionally distinct argonaute complexes after production by *dicer-1*. *Cell* 130, 287–297.

Ghildiyal, M., Seitz, H., Horwich, M.D., Li, C., Du, T., Lee, S., Xu, J., Kittler, E.L., Zapp, M.L., Weng, Z., and Zamore, P.D. (2008). Endogenous siRNAs derived from transposons and mRNAs in *Drosophila* somatic cells. *Science* 320, 1077–1081.

Ishizuka, A., Siomi, M.C., and Siomi, H. (2002). A *Drosophila* fragile X protein interacts with components of RNAi and ribosomal proteins. *Genes Dev.* 16, 2497–2508.

Johnstone, O., Deuring, R., Bock, R., Linder, P., Fuller, M.T., and Lasko, P. (2005). Belle is a *Drosophila* DEAD-box protein required for viability and in the germ line. *Dev. Biol.* 277, 92–101.

Kawamura, Y., Saito, K., Kin, T., Ono, Y., Asai, K., Sunohara, T., Okada, T.N., Siomi, M.C., and Siomi, H. (2008). *Drosophila* endogenous small RNAs bind to Argonaute 2 in somatic cells. *Nature* 453, 793–797.

Kim, J.K., Gabel, H.W., Kamath, R.S., Tewari, M., Pasquinelli, A., Rual, J.F., Kennedy, S., Dybbs, M., Bertin, N., Kaplan, J.M., et al. (2005). Functional genomic analysis of RNA interference in *C. elegans*. *Science* 308, 1164–1167.

Labourier, E., Adams, M.D., and Rio, D.C. (2001). Modulation of P-element pre-mRNA splicing by a direct interaction between PSI and U1 snRNP 70K protein. *Mol. Cell* 8, 363–373.

Lasko, P. (2000). The *Drosophila melanogaster* genome: translation factors and RNA binding proteins. *J. Cell Biol.* 150, F51–F56.

Lee, Y.S., Nakahara, K., Pham, J.W., Kim, K., He, Z., Sontheimer, E.J., and Carthew, R.W. (2004). Distinct roles for *Drosophila* Dicer-1 and Dicer-2 in the siRNA/miRNA silencing pathways. *Cell* 117, 69–81.

Okamura, K., Chung, W.J., Ruby, J.G., Guo, H., Bartel, D.P., and Lai, E.C. (2008). The *Drosophila* hairpin RNA pathway generates endogenous short interfering RNAs. *Nature* 453, 803–806.

Parry, D.H., Xu, J., and Ruvkun, G. (2007). A whole-genome RNAi screen for *C. elegans* miRNA pathway genes. *Curr. Biol.* 17, 2013–2022.

Saleh, M.C., van Rij, R.P., Hekele, A., Gillis, A., Foley, E., O'Farrell, P.H., and Andino, R. (2006). The endocytic pathway mediates cell entry of dsRNA to induce RNAi silencing. *Nat. Cell Biol.* 8, 793–802.

Salz, H.K., Mancebo, R.S., Nagengast, A.A., Speck, O., Psotka, M., and Mount, S.M. (2004). The *Drosophila* U1-70K protein is required for viability, but its arginine-rich domain is dispensable. *Genetics* 168, 2059–2065.

Stowers, R.S., and Schwarz, T.L. (1999). A genetic method for generating *Drosophila* eyes composed exclusively of mitotic clones of a single genotype. *Genetics* 152, 1631–1639.

Tomari, Y., Du, T., and Zamore, P.D. (2007). Sorting of *Drosophila* small silencing RNAs. *Cell* 130, 299–308.

Ulvila, J., Parikka, M., Kleino, A., Sormunen, R., Ezekowitz, R.A., Kocks, C., and Ramet, M. (2006). Double-stranded RNA is internalized by scavenger receptor-mediated endocytosis in *Drosophila* S2 cells. *J. Biol. Chem.* 281, 14370–14375.

Wang, X.H., Aliyari, R., Li, W.X., Li, H.W., Kim, K., Carthew, R., Atkinson, P., and Ding, S.W. (2006). RNA interference directs innate immunity against viruses in adult *Drosophila*. *Science* 312, 452–454.

Zamore, P.D., and Haley, B. (2005). Ribo-gnome: the big world of small RNAs. *Science* 309, 1519–1524.

(C) Small RNAs are enriched in the *Bel* and ribosomal protein immunoprecipitates. Expression constructs for FLAG-tagged proteins together with that for the CXCR4 siRNA mimetic were transfected into S2-NP cells. Total RNA was extracted from FLAG immunoprecipitates and subjected to northern blotting using probes against Bantam, esi-2.1, and CXCR4. To avoid signal saturation, ~25% of the RNA recovered from the Ago1 and Ago2 samples was loaded compared to the rest of the samples. Total RNAs recovered from 10% of the cell extracts were processed in parallel as input control.